

2,5-Diamino-1,4-benzoquinones: Promising candidates against HT-29 human colorectal cancer cell line and as HSP90 inhibitors

Asha A

Department of Chemistry, Baby John Memorial Government College, Chavara, Kollam 691 583, India

E-mail: ashaiqacbjm@gmail.com

Received 1 November 2024; accepted (revised) 27 December 2024

Herein is reported the synthesis of seven 2,5-diamino-1,4-benzoquinones to act as potent anti-cancer agents against HT-29 human colorectal adenocarcinoma cell line *via* MTT assay, fluorescence microscopy and flow cytometric assays. All the aminobenzoquinones show promising activity and 2,5-dibenzylamino-1,4-benzoquinone exhibits best results (IC₅₀ 12.5 µg/mL). Fluorescence microscopic and cell cycle analysis have been carried out to study the pathway of their activity. Molecular docking analysis using Schrodinger software have been carried out to study the ability of these compounds to act as HSP90 inhibitors.

Keywords: Aminobenzoquinones, Fluorescence microscopy, Flow cytometry, Molecular docking, HSP90 Inhibitor

The uncontrolled growth of genetically changed cells in organisms results in cancer, the second leading cause of global death as per the statistics of World Health Organization. Prostate and breast cancer leads the list in male and female respectively followed by lung and colon cancer¹. Chemotherapy, radiation therapy, immunotherapy, and targeted therapy remains the regular treatment strategies apart from surgery. Use of anti-cancer drugs and drug combinations to prevent and treat cancer has been gaining acceptance in the current scenario. The development of chemotherapeutic strategies involving novel small molecule anti-tumour agents has therefore been the focus area of cancer chemotherapy for several decades to combat and control the incidence of cancer.

Aminobenzoquinones are effective anti-cancer agents which date back to the discovery of Mitomycin C and the activity is essentially due to DNA damage by covalent bond formation which is different from that of anthraquinone drugs in which planarity results in an effective intercalation of the compound with the base pairs of nucleic acids². The mode of action of mitomycin C and saframycins A and C undoubtedly implies the involvement of amino part which is the site of attachment of the drug to the nucleic acid base. Owing to its ability to undergo deprotonation, aminobenzoquinones can act as electrophiles which can effectively bind with the nucleophilic sites in the base. Cannabinoid, HU-331 was shown to be highly

effective against human cancer cell line HT-29 and in Raji lymphoma both *in vitro* and *in vivo*³. The significant anti-cancer potency cyclohexylamine substituted isoquinolinequinones on lung and bladder cell lines has been reported⁴. The protein target of benzoquinone derived anti-cancer agents is found to be Hsp-90, an important protein chaperon in mammalian cells⁵⁻⁹. The ROS production by the anti-cancer agents is accountable for apoptosis induction in different types of cancer including colon cancer and leukemia¹⁰⁻¹⁵. The discrete ability of quinone ring to undergo reduction to produce semiquinone radical anion makes them capable to interact with DNA¹⁶. Thus, quinone drugs with more negative potential may be effective anti-cancer agents. The generation of Reactive Oxygen Species (ROS) during the redox process of quinones can cause strand break in DNA which is due to the absence of protecting enzymes in tumor cells and make the compound potent chemotherapeutic agent¹⁷. Introduction of various amino groups in quinone ring can thus result in the production of excellent anti-cancer agents owing to their varied reduction potential. More negative reduction potential can enhance quinone methide formation which in turn can be achieved by the introduction of electron rich substituents in quinone ring. You *et al.* proved that 2,5-bis-(cyclohexylamino)-1, 4-benzoquinone possess urease inhibitory activity¹⁸.

Heat shock protein HSP90 is one of the most important targets for the development of quinone anti-cancer agents against many cancer cell lines especially colorectal cancer¹⁹. HSP90 is a human molecular chaperon critical for folding and conformational stability of many client proteins which promote the growth of cancer cells. HSP90 inhibition imparts degradation of a set of proteins like p53, Her-2/ErbB2, c-Raf-1 and Cdk4 involved in the progression of cancer²⁰. Benzoquinone ansamycin antibiotics like geldanamycin, herbimycin A and 17-Allylamino-17-demethoxygeldanamycin (17-AAG) are reported as effective HSP90 inhibitors^{21,22}. Ansamycin antibiotics like 17-AAG bind with the ATP-binding site in the N-terminal domain of HSP90 and thus inhibits folding and ATPase activity leading to cell cycle disruption²³. In tumour cells HSP90 exist in a complexed high-affinity form with high ATPase activity which is responsible for its 100-fold greater affinity for 17-AAG than normal HSP90²⁴. Since ABQs possess structural similarity with benzoquinone ansamycins, we have studied their ability to act as HSP90 inhibitors by molecular docking.

Materials and Methods

MTT assay

The *in vitro* anti-cancer activity of the synthesized ABQs were carried out by MTT (3-(4, 5-dimethyl thiazol-2-yl)-2, 5-diphenyl tetrazolium bromide) assay in HT-29 (human colorectal adenocarcinoma) cell. The cell line procured from National Centre for Cell Sciences (NCCS), Pune, India was cultured in 25 cm² tissue culture flask with DMEM supplemented with 10% FBS, L-glutamine, sodium bicarbonate and antibiotic solution containing: Penicillin (100U/mL), Streptomycin (100µg/mL), and Amphotericin B (2.5µg/mL). Cultured cell lines were kept at 37°C in a humidified 5% CO₂ incubator (NBS Eppendorf, Germany). The viability of cells were evaluated by direct observation of cells by Inverted phase contrast microscope and followed by MTT assay method. Two days old confluent monolayer of cells were trypsinized and the cells were suspended in 10% growth medium, 100 µL cell suspension (5×10⁴ cells/well) was seeded in 96 well tissue culture plate and incubated at 37°C in a humidified 5% CO₂ incubator. 1 mg of ABQ was completely dissolved in 1 mL of 5% DMEM using cyclomixer. The compound solution was then filtered through 0.22 µm Millipore syringe filter to ensure the sterility. After 24

hours the growth medium was removed, freshly prepared each compound in 5% DMEM were five times serially diluted by two-fold dilution (100, 50, 25, 12.5, 6.25µg in 100 µL of 5% MEM) and each concentration of 100 µL were added in triplicates to the respective wells and incubated at 37°C in a humidified 5% CO₂ incubator. Entire plate was observed after 24 hours of incubation in an inverted phase contrast tissue culture microscope (Olympus CKX41 with Optika Pro5 CCD camera) and microscopic observation were recorded as images. After 24 hours of incubation period, the sample content in wells were removed and 30 µL of reconstituted MTT solution was added to all wells containing test and control cells, the plate was gently shaken, then incubated at 37°C in a humidified 5% CO₂ incubator for 4 hours. After the incubation period, the supernatant solution was removed and 100 µL of MTT solubilization solution [DMSO] was added and the wells were mixed gently by pipetting up and down in order to solubilize the formazan crystals. The absorbance values were measured by using micro plate reader at a wavelength of 540 nm²⁵. IC₅₀ value was calculated using ED₅₀ PLUS V1.0.

Fluorescence Microscopic examination

Morphological detection of apoptotic and necrotic cells was carried out by Acridine Orange/ Ethidium Bromide double staining method. After treating the cells with 12.5 µg/mL of the more active ABQ for 24 h, the cells were washed with cold PBS and then stained with a mixture of AO (100 µg/mL) and EB (100 µg/mL) at RT for 10min. The stained cells were washed twice with 1X PBS and observed under fluorescence microscope in blue filter of fluorescent microscope Olympus CKX41 with Optika Pro5 camera.

Flow cytometry

HT-29 cells were cultured as per standard procedures and treated with 12.5µg/mL of BAPBQ for 24 hours. The cell sample was transferred to a 12×75mm polystyrene tube or 50 mL conical flask. The samples were then centrifuged at 3000rpm for 5minutes. The supernatant solution was removed without disturbing the pellet. After centrifugation, the cell pellet forms a visible pellet on the bottom of the tube.

Appropriate volume of PBS was added to each tube (*i.e.*, 1 mL of PBS per 1×10⁶ cells) and the contents were mixed by pipetting several times and gently

vortexing. The cells were centrifuged at 3000rpm for 5 minutes. The supernatant solution was discarded without disturbing the cell pellet, leaving approximately 50 μL of PBS per 1×10^6 cells. The pellet was resuspended in the residual PBS by repeated pipetting several times and gently vortexing. The resuspended cells were added drop wise into the tube containing 1 mL of ice cold 70% ethanol while vortexing at medium speed. The tube was capped and frozen at -20°C . After the overnight incubation, the samples were centrifuged at 3000rpm for 5 minutes at RT. The supernatant solution was removed and 250 μL PBS was added to the pellet. Then the centrifugation was done again at the same rpm and time. The pellet was taken after discarding the supernatant solution and 250 μL of cell cycle reagent was added. This was incubated at dark for 30 minutes (which is light sensitive). After this, it was analyzed using a Flow Cytometer. Gating was performed with reference to untreated control cells and samples were analyzed.

Molecular docking

Docking simulation was carried out using Maestro 9.2 version software (Schrodinger LLC suite, 2015) installed in single machine running on core TM Duo processor with 2GB RAM and 180 GB with Centro Linux as the operating system.

Protein preparation

The crystal structure of HSP90 molecular chaperon (PDB ID: 3R91, Resolution = 1.579 \AA) was retrieved from RCSB protein bank. The protein was preprocessed by adding polar hydrogen and water molecules were retained as they stabilize the ligand in the active site^{26,27}. The ionization ($p\text{H}$), optimization of hydrogen bond and restorative energy minimization steps were applied in order to correct the geometry of receptor protein.

Ligand library

The ABQs were first drawn in Chem Sketch and exported as mol files to Maestro, 9.2 version of Schrodinger software. The ligands were then prepared by ligprep to generate an energy minimized 3D conformation.

The grid map for the receptor protein was generated by receptor grid generation panel around the active site of the internal ligand. Once the receptor grid is generated, the ligands are docked to the protein

(3R91) using Glide version 5.8 (Grid based Ligand Docking with Energetics). Extra precision (XP) glide docking, a powerful sampling protocol was applied for docking which specifies only good ligand poses [Schrodinger, LLC, Glide, v.5.6. Schrodinger LLC, New York, 2010c].

ADME property analysis

QikProp tool of Schrodinger suite was used to analyze the ADME properties of the ligands which predicts the physiochemical properties with a detailed analysis of: (i) predicted IC_{50} value for blockage of HERG K^+ channels (ii) Caco-2 cell permeability (iii) brain/blood partition coefficient (iv) apparent MDCK cell permeability (v) prediction of binding to human serum albumin and (vi) percentage of human oral absorption.

Results and Discussion

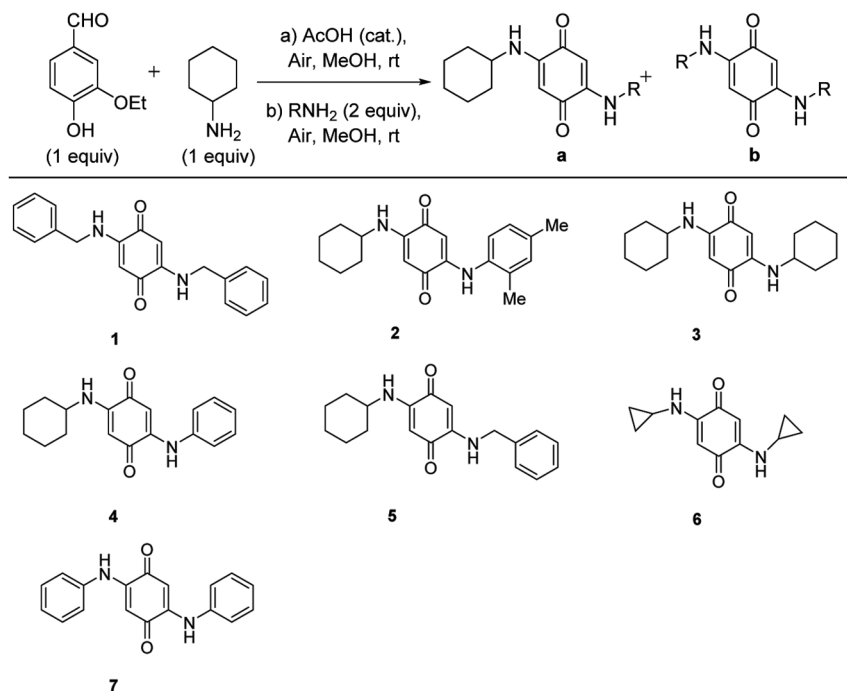
Synthesis

Seven ABQs were synthesized as per the reported procedure²⁸ (Scheme 1).

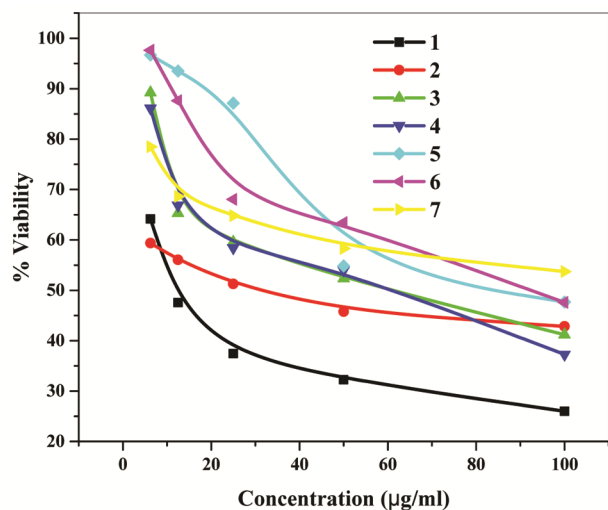
MTT Assay

All the ABQs show significant anti-cancer activity as all of them produced detectable changes in the morphology of the cells, such as shrinking of cells, granulation and vacuolization in the cytoplasm of the cells as shown in Figure S1 – S7.

Fig. 1 demonstrates a correlation between percentage viability of cancer cell lines with varying concentration of ABQs. The IC_{50} values are shown in Fig. 2. Among all the ABQs studied, **1** which is the benzylamino substituted has the maximum activity with an IC_{50} 12.5 $\mu\text{g}/\text{mL}$. There is a sharp decrease in activity on replacing one of the benzylamino group by cyclohexylamino group as in **5**, (IC_{50} -85.0 $\mu\text{g}/\text{mL}$). But if the benzylamino group in **5** is replaced by 2, 4-dimethylanilino group as in **2**, activity, is increased with an IC_{50} - 45.1 $\mu\text{g}/\text{mL}$. If the bulky methyl anilino group is replaced by cyclohexylamino as in **3**, activity decreases (IC_{50} -60.4 $\mu\text{g}/\text{mL}$). Minimum activity is observed in **6** (IC_{50} - 86.5 $\mu\text{g}/\text{mL}$) with the comparatively lower alkyl group attached to N-atom. This clearly indicates that attaching bulkier alkyl group like benzylamino to the N-atom in aminobenzoquinones can significantly enhance the antitumor activity. This observation is further confirmed by the docking study presented in the following session. **3** and **4** shows comparable activity

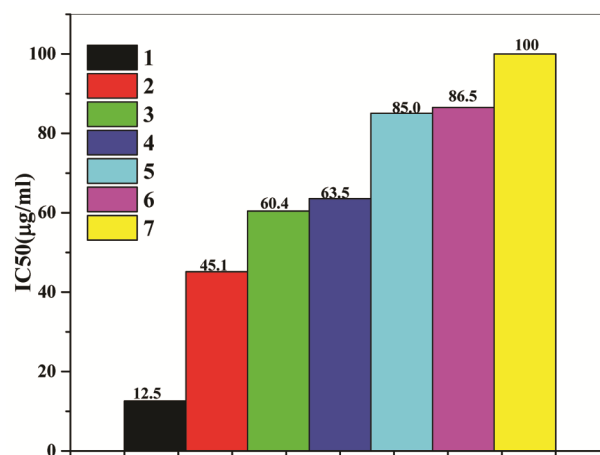


Scheme 1 — Synthesis of the aminobenzoquinones (ABQ)

Fig. 1 — Variation of % viability of cancer cells with varying concentration ($\mu\text{g/mL}$) of ABQs

which is attributed to the fact that aniline and cyclohexylamine does not differ much in terms of bulkiness. The low activity of **7** is specifically due to its poor solubility in DMSO which is a deviation of our docking study where it shows better docking score next to **3**. Desolvation cost seems to be the cause of why some ligands that seem to fit into a binding site cannot experimentally be confirmed to be inhibitors²⁹.

To understand whether the compounds are specially targeting the cancer cells rather than normal

Fig. 2 — IC₅₀ values of ABQs in $\mu\text{g/mL}$

cells, we studied the effect of the compounds on inhibiting cell growth in HEK 293 (human embryonic kidney cells) cell line. The percentage viability was in the range 75-80 for all the ABQs at corresponding IC₅₀ concentration as shown in Table 1 which proves the non-toxicity of ABQs towards normal cells.

Fluorescence microscopic examination for apoptosis

Apoptosis is an essential type of cell death in multicellular organisms, the insufficiency of which results in uncontrolled cell proliferation like that in cancer. The chemotherapeutic action of agents like

Mitomycin C and Adriamycin is mediated by apoptosis, which points towards the significance of the process.

Since MTT assay revealed **1** as the most potent anti-cancer agent among our ABQs, we executed fluorescence microscopic examination with it to investigate qualitatively the occurrence of apoptosis. DNA-binding dyes Acridine Orange (AO) and Ethidium Bromide (EB) were used for the morphological detection of apoptotic and necrotic cells³⁰. AO is taken up by both viable and non-viable cells and emits green fluorescence if intercalated into double stranded nucleic acid (DNA). EB is taken up only by non-viable cells and emits red fluorescence by intercalation into DNA. HT-29 cells with normal morphology had normal green nuclei, while **1** treated cells showed bright green nucleus with condensed or fragmented chromatin indicating apoptosis. Chromatin condensation and fragmentation leads to intercalation of ethidium bromide there by resulting in orange-stained cell nuclei (orange fluorescence). Cell shrinkage, membrane blebbing and chromatin condensation which are the characteristics of apoptosis were observed in **1** treated cell under phase contrast microscope. Fig. 3 shows the morphological changes of HT-29 cells treated with **1** at its IC₅₀ concentration (12.5 µg/mL) and 25 µg/mL. Thus, double staining study shows that ABQs possess anti-cancer property which is mediated by induction of apoptosis.

Table 1 — IC₅₀ and % viability of ABQs against HEK293 human embryonic kidney cells

ABQ	IC ₅₀ (µg/mL)	Viability (%)
1	12.5	76.17
2	45.1	75.88
3	60.4	74.65
4	63.5	70.92
5	85.0	71.21
6	86.5	70.01
7	100	75.20

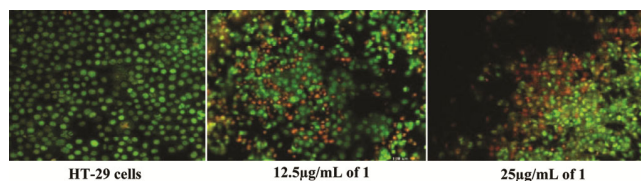


Fig. 3 — Fluorescent micrograph of HT29 cells after AO/EB staining showing live, early apoptotic and late apoptotic cells. (a) Untreated HT29 cells, (b) cells treated with 12.5 µg/mL of **1**, (c) cells treated with 25 µg/mL **1**.

Cell cycle analysis by flow cytometry

Flow cytometry is a widely used technique which allows multiparametric analysis of the physical and chemical characteristics of a population of cells or particles. One of the major applications of this technique include the characterization and isolation of rare cells types like adult stem cells and cancer initiating cells as it provides the distribution of nuclei based on their DNA content³¹⁻³³. The other applications include determination of cell size, apoptosis, cell cycle, DNA synthesis, cell proliferation, cell sorting, *etc.*

The more active aminobenzoquinone **1** was selected for the study.

Monitoring a cell's ability to proliferate is critical for assessing a cell's health during toxicity studies. The most accurate method of doing this is by directly measuring DNA synthesis. The basic principle of MUSE cell cycle kit is a standard ethanol fixation and detergent permeabilization which is sufficient to gain access to the DNA during active cell cycle. The kit utilizes a premixed reagent which includes the nuclear DNA intercalating stains Propidium iodide (PI) which discriminates cells at different stages of the cell cycle based on the differential DNA content in the presence of RNAase to increase the specificity of DNA staining in each phase (G0/G1, S and G2/M). Flow cytometry was used to analyze the cell cycle distribution of HT-29 cells 24h after treatment with 12.5 µg/mL of the compound **1**. It found to arrest the cell cycle at G0/G1 phase since the percentage of cell cycle distribution was higher in G0/G1 phase. Also, the percentage of cell cycle distribution was less in S and G2/M phase indicating that **1** has significantly changed the ratio of cell distribution. Increase in cell distribution results in cell arrest. It is clear that the % of cells distributed in G0/G1 phase increased to 82.5%. The cell distribution was seen to be decreased in S phase and G2/M phase. From Fig. 4, it is clear that the percentage of inhibition is higher in G0/G1 phase and hence the results suggest that **1** can be used as G0/G1 regulator.

Molecular docking

HSP90, a chaperon protein playing key role in protein degradation and act as stabilizer for tumor growth has emerged as a promising target for the development of anticancer agents as it is over expressed in malignant cells. Among a number of molecular chaperones for cell viability, only HSP90 has shown to possess differential activity in normal

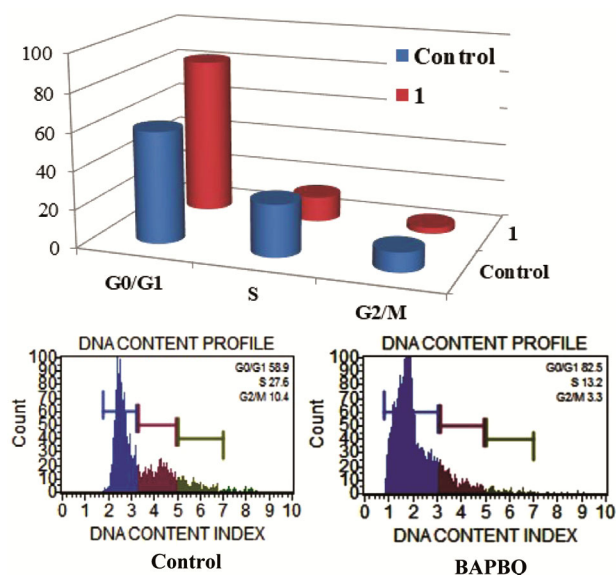


Fig. 4 — Effect of 1 on the cell cycle in HT-29 cells as DNA content index

vs. cancerous cells³⁴. Nearly 50% of identified HSP90 dependent client proteins are directly related to oncogenesis³⁵. Moser *et al.* has inferred that HSP90 inhibitors can irreversibly bind with the chaperone from malignant cells than from normal cells with great affinity³⁶ while Tillotson *et al.* developed a novel method to assess the level of drug occupancy on Hsp90 after Hsp90 inhibitor treatment *in vitro* and *in vivo*³⁷. Drecoll *et al.* reported that the proliferative potential of malignant cells depends on HSP90 activity which promotes apoptotic death of cancer cells³⁸. As per the reports of Kelland *et al.*, elevated HSP90 expression levels were detected in human colon carcinomas which suggest HSP90 inhibition as multi-aspect treatment strategy³⁹. Geldanamycin and Herbinmycin which are benzoquinone ansamycins exhibit anti-cancer activity by binding to HSP90 *via* its N-terminal ATP binding site⁴⁰. In addition, 17 AAG, an allylamino and demethoxygeldanamycin derivative has entered in phase I clinical trial in cancer as first-in-class HSP90 inhibitor owing to its novel mode of action and better therapeutic index. Thus, HSP90 inhibition is gaining significance in cancer treatment and since aminobenzoquinones possess structural similarity with ansamycins, we investigated the ability of our ABQs to act as potent HSP90 inhibitors. As molecular docking remains a powerful approach for structure-based drug discovery, we carried out docking study of ABQs with an HSP90 protein target (PDB ID: 3R91). In a recent study, Zhicheng *et al.* has proved that HSP90

inhibition effectively decreases the proliferation and induces apoptosis in HT-29 human colon cancer cell lines⁴¹, meanwhile the molecular mechanism involved in HSP90 inhibited apoptotic pathway is seldom reported. In this context, we have selected an HSP90 protein 3R91 (Resolution- 1.579Å) for molecular docking study.

All the synthesized ABQs show a better interaction in terms of docking scores reflecting drug binding affinities with 3R91. All of them satisfy Lipinski's rule of 5 and ADME profile. Binding affinities of the ABQs with 3R91 were analyzed and evaluated based on the docking score and the number of intermolecular hydrogen bonding interactions of the resulting receptor-ligand complexes. Since the anti-cancer activity of ABQs is related with the nature of NH attached to benzoquinone moiety as per MTT assay, they show the same trend in its interaction with the protein 3R91.

Compound 6 with only 3 carbon atoms in the alkyl part is found to have the least docking score of 6.797 which increases to 8.398 when the alkyl group is cyclohexyl. This observation can be correlated with the increased cytotoxic activity of substituted 1, 4-naphthoquinones with the increase in chain length of terpenyl substituents. The longer terpenyl moiety in these compounds enhances their cell membrane permeability and bioavailability which in turn increases their cytotoxic activity. Presence of benzylamino group significantly enhances the anti-cancer activity of ABQ as is evident from docking score (8.901). The correlation between docking score and IC₅₀ of ABQs shows a deviation in the case of 7 which is in regard to its poor solubility.

The strength of protein-ligand interaction is determined by the free energy of binding which is the experimental expression of docking scores in *in silico* approach. The binding free energy (Kcal/mol) of the ligands with the receptor protein along with docking scores is shown in Fig. 5. It is obvious that the binding energy of all the ABQs except 7 is better than that of the standard drug Streptonigrin (-38.864 Kcal/mol). Again, 1 has the most favorable conformation and hence the highest binding free energy -63.050 Kcal/mol considerably better than the standard drug.

Biological recognition processes are specifically in terms of H-bonding. Existence of hydrogen bonds with significant bond length between protein and ligand remains the focus of activity of many anti-cancer drugs^{42,43}. H-bond with aromatic ring acting as

π acceptor has been reported by many researchers^{44,45}. Despite the fact that these interaction between NH donors and aromatic side chains are observed rarely and usually at long distances (>3.5 Å) in proteins, there are cases where ligand phenyl rings accept hydrogen bonds from protein amide NH groups^{46,47}. This kind of interaction between the phenyl ring and Phe138 amino acid residue in 3R91 plays a crucial role in the enhanced activity of **1** compared to other ABQs. **5** and **2** similarly shows aromatic π -protein interaction with LYS58 & TYR139 respectively. Hydrophobic interaction between amino acid residue in the protein and cyclohexylamino group adds to the activity of **2**. Quinone oxygen in **7** & **6** forms H-bonds with LEU107 & TYR139 residues (2.08 & 2.25 and 2.16Å) while a H-bonding network involving structural water molecules and amino acid residue is visible in **4**. **3** also interact with the protein *via* H-bonding between one of the quinone oxygen atom in hydroxy form with LEU 107 (Fig. 6).

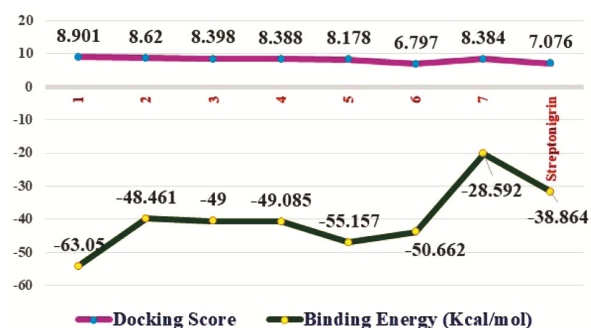


Fig. 5 — Docking scores and binding energy of ABQs in comparison with Streptonigrin

Protein-ligand interactions are often mediated by water molecules situated in deep grooves in the binding site which can be considered as part of the protein structure and forms multiple hydrogen bonds with both binding partners⁴⁸. The ligand interaction between the ABQs and the protein are depicted in Fig. 7. In all the ABQs, specific H-bonding exists between oxygen and nitrogen donor sites with amino acid residue in the protein. Structural water molecule act as a link between **1** and amino acid residue of protein through H-bonding involving quinone oxygen atom which is evident from the docking picture given in Fig. 8. The qikprop results of all ABQs confirm their drug likeness, which is more convincing in the case of **1**. So, in overall view, aminobenzoquinones with varying amino substituents can be developed as potential anti-cancer drugs *via* HSP90 inhibition.

ADME prediction of pharmacokinetic properties

The physiochemical properties of the synthesized ABQs were calculated by the Qikprop tool of Schrodinger maestro 9.2 version and the results are presented in Table 2. Human colon carcinoma (Caco-2) is the most popular high-throughput screening tool for drug permeability. The Caco-2 permeability of all the ABQs is in the range 720-1600nm/S which is much better than the standard requirement (500nm/S). This shows that all the ABQs possess human intestinal permeability which is an essential criterion for an anti-cancer drug. Moreover, the molecular mass of all the ABQs are less than 500 expecting easy transportation and absorption. The %

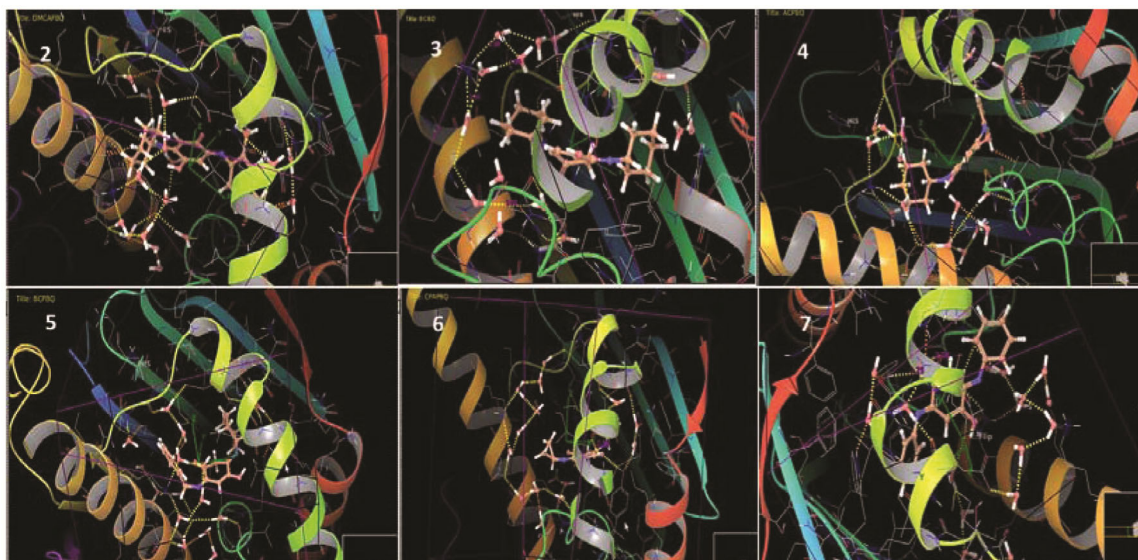


Fig. 6 — 3D interaction diagram of ABQs with protein (PDB ID: 3R91) showing H-bonding network

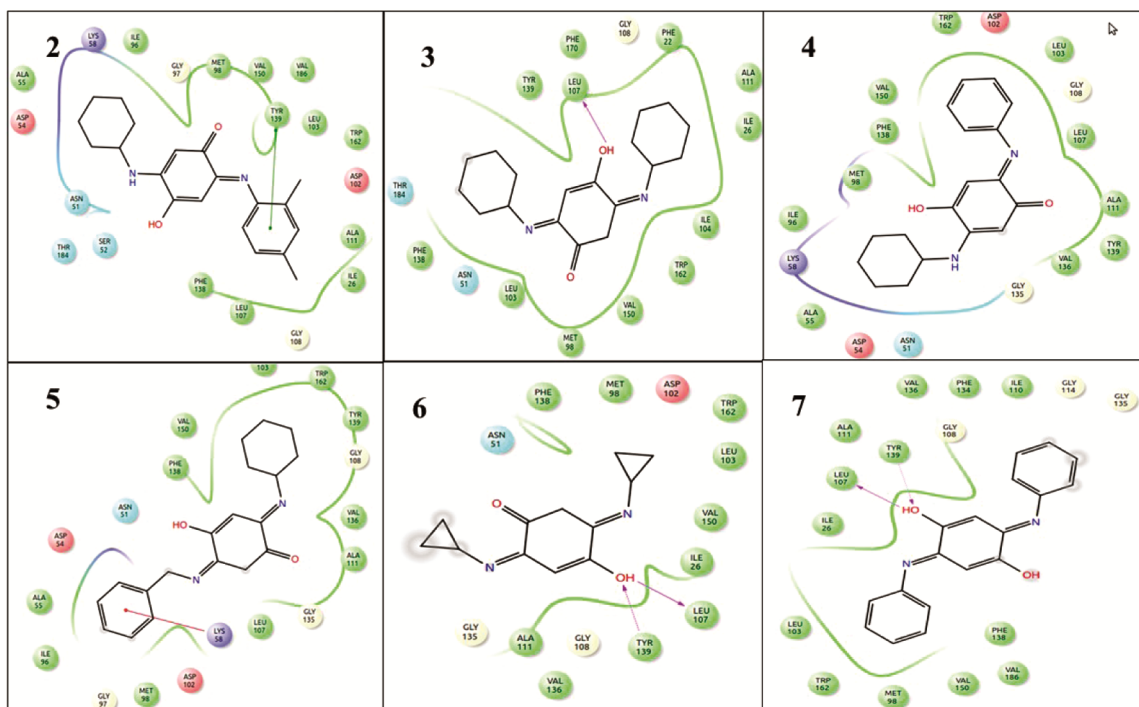


Fig. 7 — Ligand interaction between ABQs and protein (PDB ID: 3R91)

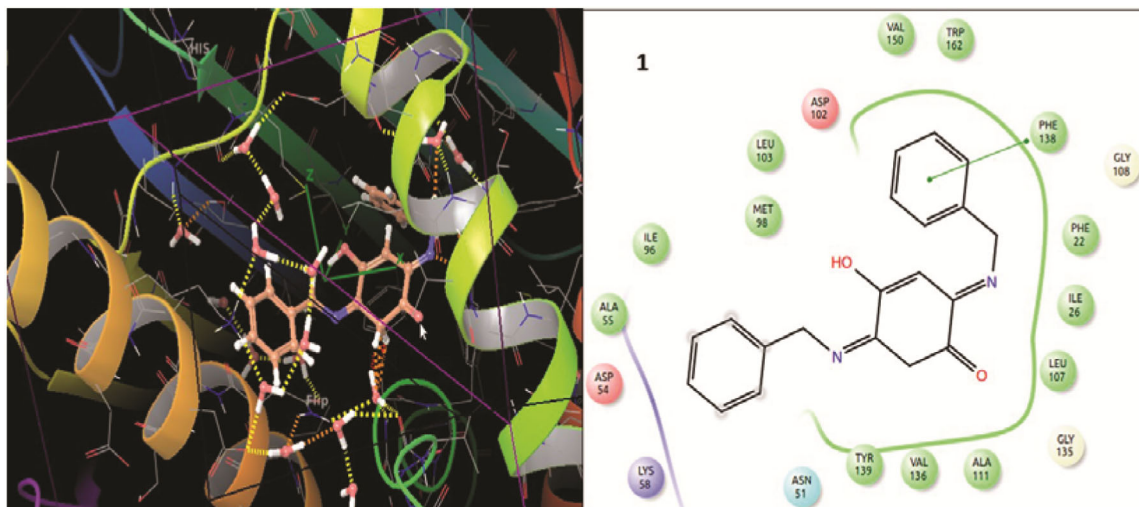


Fig. 8 — (a) 3D interaction diagram of **1** with protein (PDB ID: 3R91) showing H-bonding network involving quinone oxygen atom and lattice water molecules (yellow dotted lines) and, (b) ligand interaction in **1** between the phenyl ring and PHE138 amino acid residue.

human oral absorption of all the compounds ranges from 90-100% designating good bioavailability. The number of hydrogen bond donors and acceptors of all the compounds are less than 5 and 10 respectively as required for a drug candidate. The topological polar surface area (TPSA) of a drug molecule decides its ability to permeate tumor cells and penetrate the blood-brain barrier. TPSA less than 90 angstrom squared is an essential criterion for an effective drug

which is satisfied by all of our compounds as their values ranges from 63 to 71 angstrom squared. In addition, all the ABQs satisfy Lipinski's rule of five which makes them orally active.

Experimental Section

General procedure for synthesis of ABQs

Ethyl vanillin (10 mmol) and cyclohexylamine (10 mmol) were mixed in 10 mL methanol along with

Table 2 — Molinspiration calculation of drug-likeness of ABQs

ABQ	Mol.wt	QPP Caco (nm/S)	H-bond acceptor	H-bond donor	No of rotating bonds	Percent Human Oral Absorption (%)	TPSA	Lipinski's violation
Rules	<500	>500	<10	<5	<10	>80	<90	0
1	318.374	1578.07	4.75	1	4	100	64.501	0
2	324.422	725.134	4.75	2	5	100	71.928	0
3	302.416	1607.15	4.75	1	5	100	63.457	0
4	296.368	919.045	4.75	2	5	100	68.975	0
5	310.395	1331.21	4.75	1	6	100	68.236	0
6	218.255	967.611	4.75	1	5	90.86	68.019	0
7	290.321	720.605	3.5	2	6	96.83	64.663	0
Streptonigrin	506.471	4.407	12.5	5.5	9	6.12	214.912	3

addition of a trace amount of glacial acetic acid and allowed for slow evaporation under open air at RT. After complete evaporation of methanol, the resulting residue was redissolved in 10 mL of methanol and two equivalents of aromatic/alicyclic primary amines added and the solvent allowed to evaporate in open air at RT. Complete evaporation of the solvent followed by purification of the residual reaction mass by column chromatography over silica gel using hexane/ethyl acetate gradient afforded ABQs.

2,5-Dibenzylamino-1,4-benzoquinone, 1:

¹H NMR (DMSO-*d*₆): δ 4.37 (d, *J* = 8 Hz, 4H), 5.17 (s, 2H), 7.10-7.48 (m, 10H), 8.26 (m, 2H); ¹³C NMR (DMSO-*d*₆): δ 45.1, 79.0, 93.2, 127.1, 127.2, 128.5, 137.2, 151.0, 177.7; HR-ESI-MS: *m/z* Calcd for C₂₀H₁₉N₂O₂ [M+H]⁺ 319.1447. Obsd: 319.1451.

2-(2,4-Dimethylanilino)-5-cyclohexylamino-1,4-benzoquinone, 2: ¹H NMR (CDCl₃): δ 1.21-1.33 (m, 6H), 1.72 (m, 2H), 1.93 (m, 2H), 2.15 (s, 3H), 2.23 (s, 3H), 3.22 (m, 1H), 5.35 (s, 1H), 5.43 (s, 1H), 6.45 (d, *J* = 7 Hz, 1H), 6.94-7.06 (m, 3H), 7.88 (bs, 1H); ¹³C NMR (CDCl₃): δ 17.7, 21.0, 24.5, 25.4, 29.7, 31.8, 51.4, 92.9, 95.0, 124.6, 127.5, 132.0, 132.7, 133.0, 137.0, 149.1, 178.4, 179.5; HR-ESI-MS: *m/z* Calcd for C₂₀H₂₅N₂O₂ [M+H]⁺ 325.1916. Obsd: 325.1924.

2,5-Bis(cyclohexylamino)-1,4-benzoquinone, 3: ¹H NMR (CDCl₃): δ 1.18-1.42 (m, 10H), 1.59-1.69 (m, 3H), 1.74-1.83 (m, 4H), 1.94-2.02 (m, 4H), 3.26 (m, 2H), 5.33 (s, 2H), 6.59 (d, *J* = 9 Hz, 2H); ¹³C NMR (CDCl₃): δ 24.5, 25.4, 31.8, 51.3, 92.8, 150.2, 178.1; HR-ESI-MS: *m/z* Calcd for C₁₈H₂₇N₂O₂ [M+H]⁺ 303.2073. Obsd: 303.2078.

2-Anilino-5-cyclohexylamino-1,4-benzoquinone, 4: ¹H NMR (CDCl₃): δ 1.29-1.45 (m, 5H), 1.69 (d, *J* = 12.5 Hz, 1H), 1.82 (d, *J* = 12.5 Hz, 2H), 2.03

(d, *J* = 11.5 Hz, 2H), 3.32 (m, 1H), 5.46 (s, 1H), 6.0 (s, 1H), 6.51 (bs, 1H), 7.23-7.29 (m, 3H), 7.43 (t, *J* = 7.5 Hz, 2H), 8.24 (bs, 1H); ¹³C NMR (CDCl₃): δ 24.5, 25.4, 31.8, 51.4, 93.0, 95.6, 122.7, 125.9, 129.6, 137.3, 147.5, 149.2, 178.3, 180.1; HR-ESI-MS: *m/z* Calcd for C₁₈H₂₁N₂O₂ [M+H]⁺ 297.1603. Obsd: 297.1610.

2-Benzylamino-5-cyclohexylamino-1,4-benzoquinone, 5: ¹H NMR (CDCl₃): δ 1.12-1.34 (m, 7H), 1.68-1.75 (m, 2H), 1.89-1.92 (m, 1H), 3.13-3.28 (m, 1H), 4.27 (d, *J* = 6 Hz, 2H), 5.29 (d, *J* = 10.5 Hz, 2H), 6.46 (d, *J* = 7.5 Hz, 1H), 6.80 (bs, 1H), 7.19-7.30 (m, 4H), 7.25 (d, *J* = 7 Hz, 1H), 7.29 (d, *J* = 7.5 Hz, 2H); ¹³C NMR (CDCl₃): δ 24.5, 25.4, 31.8, 46.8, 51.3, 92.9, 93.7, 93.8, 127.7, 128.1, 129.0, 135.6, 149.8, 150.7, 178.1, 178.7; HR-ESI-MS: *m/z* Calcd for C₁₉H₂₃N₂O₂ [M+H]⁺ 311.1760. Obsd: 311.1766.

2,5-Bis(cyclopropylamino)-1,4-benzoquinone, 6: ¹H NMR (CDCl₃): δ 0.62-0.67 (m, 4H), 0.83-0.89 (m, 4H), 1.61 (s, 2H), 2.45-2.52 (m, 2H), 5.63 (s, 2H), 6.52 (bs, 2H); ¹³C NMR (CDCl₃): δ 7.0, 24.1, 94.9, 152.1, 179.0; HR-ESI-MS: *m/z* Calcd for C₁₂H₁₅N₂O₂ [M+H]⁺ 219.1134. Obsd: 219.1136.

2,5-Bis(anilino)-1,4-benzoquinone, 7: ¹H NMR (DMSO-*d*₆): δ 5.44 (s, 1H), 5.67 (s, 1H), 7.23 (m, 2H), 7.35 (m, 4H), 7.43 (t, *J* = 10 Hz, 4H), 8.23 (s, 1H), 9.27 (s, 1H); ¹³C NMR (solid state): δ 123.8, 125.5, 127.6, 129.4, 139.9, 147.7, 151.3, 181.5. HR-ESI-MS: *m/z* Calcd for C₁₈H₁₃N₂O₂ [M-H]⁻ 289.0977. Obsd: 289.0995.

Conclusion

In conclusion, we have synthesized aminobenzoquinones which possess significant anti-cancer activity against human colorectal adenocarcinoma (HT-29) cell lines. IC₅₀ values show that the activity of ABQs undoubtedly varies with the

nature of substituted amino group. **1** with two benzyl amino substituents at 2 and 5 positions of *p*-benzoquinone moiety shows the maximum activity followed by **2**. The bulkier the group attached; more will be the activity which is due to apoptosis as indicated by AO/EB double staining method. Moreover, the compounds are least toxic to normal cell lines. Flow cytometric analysis clearly shows that sufficient cell cycle arrest occurs after 24 hours of treatment. The binding characteristics of ABQs with human chaperon protein HSP90 (PDB: 3R91) was studied by molecular docking. Benzyl amino substituted ABQ possess best binding with the protein which shows that they can act as HSP90 inhibitors which turns to be the most efficient treatment strategy for colon cancer in the present decade. **7** shows deviation which is attributed to desolvation. All the ABQs obey Lipinski's rule to become a "drug-like" molecule with ~100% human oral absorption. The *in vitro* and *in silico* studies of ABQs can be extended to *in vivo* studies and these compounds could be further explored as potent anti-cancer drugs.

Supplementary Information

Supplementary information is available in the website
<http://nopr.niscpr.res.in/handle/123456789/58776>.

References

- Wong, M C S, Goggins W B, Yip B H K, Fung F D H, Leung C, Fang Y, Wong S Y S & Ng C F, *Sci Rep*, 7 (2017) 15698
- Pullman B, *Int J Quan Chem Quan Bio Sym*, 13 (1986) 95.
- Kogan N M, Rabinowitz R, Levi P, Gibson D, Sandor P, Schlesinger M & Mechoulam R, *J Med Chem*, 47 (2004) 3800.
- Delgado V, Ibacache A, Theoduloz C & Valderrama J, *Molecules*, 17 (2012) 7042.
- Gooljarsingh L T, Fernandes C, Yan K, Zhang H, Grooms M, Johanson K, Sinnamon R H, Kirkpatrick R B, Kerrigan J, Lewis T, Arnone M, King A J, Lai Z, Copeland R A & Tummino P J, *Proc Natl Acad Sci U S A*, 103 (2006) 7625.
- Moser C, Lang S & Stoeltzing O, *Antican Res*, 29 (2009) 2031.
- Tillotson B, Slocum K, Coco J, Whitebread N, Thomas B, West K A, MacDougall J, Ge J, Ali J A, Palombella V J, Normant E, Adams J & Fritz C C, *J Biol Chem*, 285 (2010) 39835.
- Reigan P, Siegel D, Guo W & Ross D, *Mol Pharmacol*, 79 (2011) 823.
- Sydor J R, Normant E, Pien C S, Porter J R, Ge J, Grenier L, Pak R H, Ali J A, Dembski M S, Hudak J, Patterson J, Penders C, Pink M, Read M A, Sang J, Woodward C, Zhang Y, Grayzel D S, Wright J, Barrett J A, Palombella V J, Adams J & Tong J K, *Proc Natl Acad Sci U S A*, 103 (2006) 17408.
- Lin P, Li S, Wang S, Yang Y & Shi J, *J Nat Prod*, 69 (2006), 1629.
- Zhang L, Bai Y & Yang Y, *Oncol let*, 12 (2016) 2840.
- Qian X, Li J, Ding J, Wang Z, Duan L & Hu G, *Biochem Pharm*, 76 (2008) 1705.
- Xiao D, Powolny A A & Singh S V, *J Biol Chem*, 283 (2008) 30151.
- Pan M H, Gao J H, Lai C S, Wang Y J, Chen W M, Lo C Y, Wang M, Dushenkov S & Ho C T, *Mol Carcinog*, 47 (2008) 184.
- Feng R, Ni H M, Wang S Y, Tourkova I L, Shurin M R, Harada H & Yin X M, *J Biol Chem*, 282 (2007) 13468.
- Iyer V N & Szybalski W, *Science*, 145 (1964) 55.
- Povis G, Svingen B A & Appel P, *Mol Pharm*, 20 (1981) 387.
- You Z L, Xian D M, Zhang M, Cheng X S & Li X F, *Bioorg Med Chem*, 20 (2012) 4889.
- Kushtrim K, Jarle B, Tormod K G, Anita S & Ragnhild A L, *Biochimica Biophys Acta (BBA) - Rev Can*, 1871 (2019) 240.
- Rebecca A Z, Grace A M, Christine Q & Daniel F J, *Semi Cell Dev Bio*, 88 (2019) 21.
- Alejandro A P, Rosarie A T, Carley G S, Luis G V B, Brian D L, Peter J T, Nicholas D G & Joseph Z, *J Clin Invest*, 129 (2019) 744.
- Smith R E & Davis W R, *Anal Chem*, 56 (1984) 2345.
- Sona T, Hassan M, Asadollah A, Abolfazl A, Roghayeh S & Nosratollah Z, *Chem Biol Drug Des*, 93 (2019) 760.
- Adeela K, Lia T, John S, Lin Z, Marcus F B, Lawrence C F & Francis J B, *Nature*, 425 (2003) 407.
- Laura B T, Rosiane G, Zibetti M, Paula C S, Faria Luis A S, Maria E R D, Miguel D N, Carlos A P & Elsa B D, *Int J Biol Macromol*, 34 (2004) 63.
- Ladbury J E, *Chem Biol*, 3 (1996) 973.
- Poornima C S, Dean P M, *J Comput -Aided Mol Des*, 9 (1995) 513.
- Asha A, Jaice R, Suma S, Suresh C H & Ravi S L, *Chem Sel*, 5 (2020) 2545.
- Talhout R, Villa A, Mark A E & Engberts J B F N, *J Am Chem Soc*, 125 (2003) 10570.
- Zhang J H, YU J, Li W X & Cheng C P, *Chin J Phys*, 41 (1998) 121.
- Darzynkiewicz Z, Traganos F, Zhao H, Halicka H D & Li J, *Cytometry A*, 79 (2011) 328.
- Darzynkiewicz Z & Zhao H, *Cell cycle analysis by flow cytometry*, (John Wiley & Sons, Ltd), 2014 p 1-8.
- Fiorani F & Beemster G T, *J Plant Mol Biol*, 60 (2006) 963.
- Kamal A, Thao L, Sensintaffar J, Zhang L, Boehm M F, Fritz L C & Burrows F J, *Nature*, 425 (2003) 407.
- Zhang H & Burrows F, *J Mol Med*, 82 (2004) 488.
- Moser C, Lang S & Stoeltzing O, *Antican Res*, 29 (2009) 2031.
- Tillotson B, Slocum K, Coco J, Whitebread N, Thomas B, West K A, MacDougall J, Ge J, Ali J A, Palombella V J, Normant E, Adams J & Fritz C C, *J Biol Chem*, 285(2010) 39835.
- Drecoll E, Nitsche U, Bauer K, Berezowska S, Slotta-Huspenina J, Rosenberg R & Langer R, *Int J Colorectal Dis*, 29(2014) 663.
- Kelland L R, Sharp S Y, Rogers P M, Myers T G & Workman P, *J Nat Can Inst*, 91 (1999) 1940.
- Dandawate P, Khan E, Padhye S, Gaba H, Sinha S, Deshpande J, Swamy K V, Khetmalas M, Ahmad A & Sarkar F H, *Bioorg Med Chem Lett*, 22 (2012) 3104.
- Zhicheng Y, Ang C, Xin L, Zhiyong Z & Xin J, *Am J Trans Res*, 9 (2017) 4945.
- Gupta S D, Bommaka M K, Mazaira G I, Galigniana M D, Satya Subrahmanyam C V, Gowrishankar N L & Raghavendra N M, *Int J Biol Macromol*, 80 (2015) 253.

- 43 Tsuzuki, S, Honda, K, Uchimaru, T, Mikami, M & Tanaba K, *J Am Chem Soc*, 122 (2000) 11450.
- 44 Ottiger P, Pfaffen C, Leist R, Leutwyler S, Bachorz R A & Klopper W, *J Phys Chem B*, 113 (2009) 2937
- 45 Foloppe N, Fisher L M, Francis G, Howes R, Kierstan P & Potter A, *Bioorg Med Chem Lett*, 14 (2002) 1792.
- 46 Verhoest P R, Chapin D S, Corman M, Fonseca K, Harms F, Hou J X, Marr E S F, Menniti S, Nelson F, O'Connor R, Pandit J, Proulx-LaFrance C, Schmidt A W, Schmidt C J, Suiciak J A & Liras S, *J Med Chem*, 52 (2009) 5188.
- 47 Ladbury J E, *Chem Biol*, 3 (1996) 973
- 48 Poornima C S & Dean P M, *J Comp Aided Mol Des*, 9 (1995) 513